RSC Advances

REVIEW

View Article Online
View Journal | View Issue

Cite this: *RSC Adv.*, 2023, **13**, 26650

Recent progress in liquid metal printing and its applications

Shuting Liang, *[ab] Jie Yang,[a] Fengjiao Li, [c] Shunbi Xie, [a] Na Song[d] and Liang Hu[e]

This paper focuses on the latest research printing technology and broad application for flexible liquid metal (LM) materials. Through the newest template printing method, centrifugal force assisted method, pen lithography technology, and laser method, the precision of liquid metal printing on the devices was improved to 10 nm. The development of novel liquid metal inks, such as PVA–LM ink and ethanol/PDMS/LM double emulsion ink, have further enhanced the recovery, rapid printing, high conductivity, and strain resistance. At the same time, liquid metals also show promise in the application of biochemical sensors, photocatalysts, composite materials, driving machines, and electrode materials. Liquid metals have been applied to biomedical, pressure/gas, and electrochemical sensors. The sensitivity, biostability, and electrochemical performance of these LM sensors were improved rapidly. They could continue to be used in healthy respiratory, heartbeat monitoring, and dopamine detection. Meanwhile, the applications of liquid metal droplets in catalytic-assisted MoS_2 deposition, catalytic growth of two-dimensional (2D) lamellar, catalytic free radical polymerization, catalytic hydrogen absorption/dehydrogenation, photo/electrocatalysis, and other fields were also summarized. Through improving liquid metal composites, magnetic, thermal, electrical, and tensile enhancement alloys, and shape memory alloys with excellent properties could also be prepared. Finally, the applications of liquid metal in micro-motors, intelligent robot feet, nanorobots, self-actuation, and electrode materials were also summarized. This paper comprehensively summarizes the practical application of liquid metals in different fields, which helps understand LMs development trends, and lays a foundation for subsequent research.

Received 30th June 2023
Accepted 31st August 2023

DOI: 10.1039/d3ra04356h

rsc.li/rsc-advances

Introduction

Liquid metals (LMs) are amorphous and fluid metals. They have both liquid and metal properties and play an increasingly important role in industry, biomedicine, biosensing, and flexible devices.[1] Liquid metals have a range of advantages, including low melting points, large contact areas, and good solubility.[2] The low melting point enables them to be widely printed as inks and thus used for sensor components. At the same time, the large contact area and good solubility of liquid metals enable them to be widely used in liquid-phase catalysts with good performance. Liquid metal flexible electronic devices have flexibility, impact resistance, high efficiency, and low manufacturing costs. They have good application prospects in the field of wearable intelligent devices and robots.

This paper reviews the applications and principles of LMs in different fields over the past years. The wide application of LMs is mainly divided into the following four aspects: the preparation of biological/electrochemical/pressure sensors, the preparation of photoelectrical/hydrogen catalysts, the preparation of a variety of liquid metal composites, the preparation of driving devices, *etc.* LM could be processed and printed using laser/template printing methods, combined with the latest different formulations of LM inks.

From 2021 to 2023, there has been a significant surge in liquid metal research. The development of liquid metal printing focuses on higher precision and more advanced printing technologies. Secondly, in the printing ink research, the polymer material and liquid metal form a composite ink, so that the viscosity of the printing inks are better and stronger adhesion. Regarding sensing technology, liquid metals have been used in various applications, such as biosensors, electrochemical sensors, medical sensors, *etc.* Liquid metal sensors could be developed in the direction of flexible wearable devices for the human body and extensive human health data monitoring.

[a]*College of Chemical and Environmental Engineering, Chongqing Key Laboratory of Environmental Materials & Remediation Technologies, Chongqing University of Arts and Sciences, Chongqing 402160, PR China. E-mail: stliang@cqwu.edu.cn*

[b]*Key Laboratory of Intelligent Textile and Flexible Interconnection of Zhejiang Province, Hangzhou 310018, China*

[c]*Shenzhen Automotive Research Institute, Beijing Institute of Technology, Shenzhen 518118, PR China*

[d]*Department of Oncology, Chongqing Municipal Chinese Medicine Hospital, Chongqing 400021, China*

[e]*Key Laboratory of Biomechanics and Mechanobiology, School of Biological Science and Medical Engineering, Beihang University, Beijing, 100083, PR China*

Moreover, the direction of liquid metals as catalysts has been widely expanded to catalyze the growth of assisted 2D materials, catalyze chemical reactions of organic hydrocarbons, *etc.*, which makes their catalytic applications more extensive. With the development of technology, various kinds of functional composites could also be formed by doping different polymers with liquid metals. Meanwhile, multiple types of liquid metal motors continue to be developed. Liquid metals are expected to bring disruptive changes in electronic information, flexible electronics, biomedical, and other fields.

Research progress of liquid metal patterning

In the past years, novel liquid metal patterning and printing methods have been tried, including nanotip method,[3] stencil lithography, centrifugal force-assisted printing,[4] photoetch,[5] laser activation method,[6] and stencil printing.[7] The printing accuracy could be increased to 10 nm to 2 μm.

A high precision three-dimensional (3D) nano tensile method was used to prepare LM nanotip, using room temperature gallium alloy as material. Different morphologies, and lengths of nanotip were obtained by controlling the tensile speed at a resolution of 10 nm. The accepted nano tips have a high aspect ratio over several microns. When the vertical tensile rate is 100 nm s^{-1}, the liquid metal alloy is confined within the nanotip of about 10 nm^3 (Fig. 1a).

An injection technique based on pressurized fountain pen lithography was proposed. Liquid metal was etched onto a hard flat substrate[5] (Fig. 1b) using a glass nano straw. The inside of the nano straw was coated with gold as a sacrificial layer, which promoted wetting in the pipette hole (an inner diameter of 100–300 nm). The metal was squeezed through the hole by applying hydrodynamic pressure to the pipette joint. Long continuous (>3 mm) and narrow (1–15 μm) LM wires were formed on the silicon oxide and gold surfaces. With this sturdy platform, LM patterns could be drawn down to various substrates and geometry.

Due to the low resolution of LM printing, a template lithography printing method assisted by centrifugal force was developed. The LM-based stretchable conductor was prepared with the highest printing accuracy up to 2 μm (Fig. 1c).[4] LM patterns could be formed based on this method, and molds could be used multiple times. The selective wettability of LM to the metal pattern was removed by 4% NaOH solution. Using a rotating substrate to generate centrifugal force to remove excess printed metal, an LM pattern with micron accuracy (2–20 μm) was achieved. The substrate could include PDMS or biodegradable polymer. Liquid metal serpentine resistors and interlocking capacitors could be printed based on this method. After being stretched to 80% strain, the resistor could return to its original shape.

Using laser activation, small-scale, high-density stretchable electrons could be produced in PDMS–LM composites to form a conductive circuit (Fig. 1d).[6] The consistency and precision of the laser could be combined with the printability, strain insensitivity, and ruggedness of composite materials. And high-density stretchable electrons could be produced.

Fig. 1g shows that the polyurethane (TPU) substrate was prepared by electrostatic spinning, and liquid metal circuits were printed by stencil printing.[7] Multilayer flexible circuits, resistors, capacitors, inductors, and their composite devices were constructed by layer-by-layer repetitive assembly. These devices have good stretchability, air permeability, stability, and multilayer reconfiguration. These flexible electrons were recyclable and reconfigurable, which showed excellent application potential in flexible displays, electronic skin, and flexible devices.

The novel-developed liquid metal inks include PVA–LM ink,[8] EtOH/PDMS/LM ink,[6] and hydrogen-doped LM ink.[9] Compared with previous liquid metals, these inks have better viscoelasticity and printability.

In Fig. 1e, a printable and recycled polyethylene/liquid metal (PVA–LM) ink was developed. By introducing LM into 10 wt% PVA solution, and dispersing LM into small particles by high-speed shear, a conductive ink was prepared.[8] This ink improved the wettability of the PET substrate surface and could be printed with 3D technology. It has a conductivity of 1.3×10^5 S m^{-1}, which is highly sensitive, and generates super stable signals even after 200 cycles. The flexible sensor prepared by this ink was widely used in human movement monitoring, printing alarm system, and target locator. This ink could also be recycled in alkaline conditions, and its flexible devices are environmentally friendly and recyclable.

In Fig. 1d, ethanol/polydimethylsiloxane/liquid metal (EtOH/PDMS/LM) double emulsion inks were prepared. This ink was easily printed to a silicon substrate and featured a high conductivity of 7.7×10^5 S^{-1}, little strain resistance change, and stable cycle performance.[4] By soaking LM in ultrasonic ethanol, a single emulsion was formed. Then 2–12 vol% PDMS precursor was added to the emulsion, and a double emulsion was formed by ultrasonic. The ethanol has a low viscosity which could be used to print the double emulsion ink onto the substrate. Direct laser writing could activate this printed composite ink to form a high-resolution conductive channel.

The formation of Ga_2O_3 skin on the LM limits its electrical conductivity. Therefore, by ultrasonic treatment of toluene, PEVA (polyethylenevinyl acetate), and free radical initiator DCP (di isopropyl peroxide) with LM, hydrogen-containing LM inks could be prepared (Fig. 1f).[9] Among them, excessive hydrogen free radicals provide electrons to oxygen, filling the electronic band structure of oxide skin, making it relatively high conductivity, viscoplastic, and deformable. The circuit printed by this ink showed metallic conductivity of 2.5×10^4 S cm^{-1}, constant conductivity under 500% extended strain, excellent scratch resistance, and long-term stability. This ink could directly print a 3D circuit and an inductance strain sensor.

Research progress of liquid metal sensing

In the past year, liquid metal sensor components have been successfully implemented in healthcare, daily activity tracking,

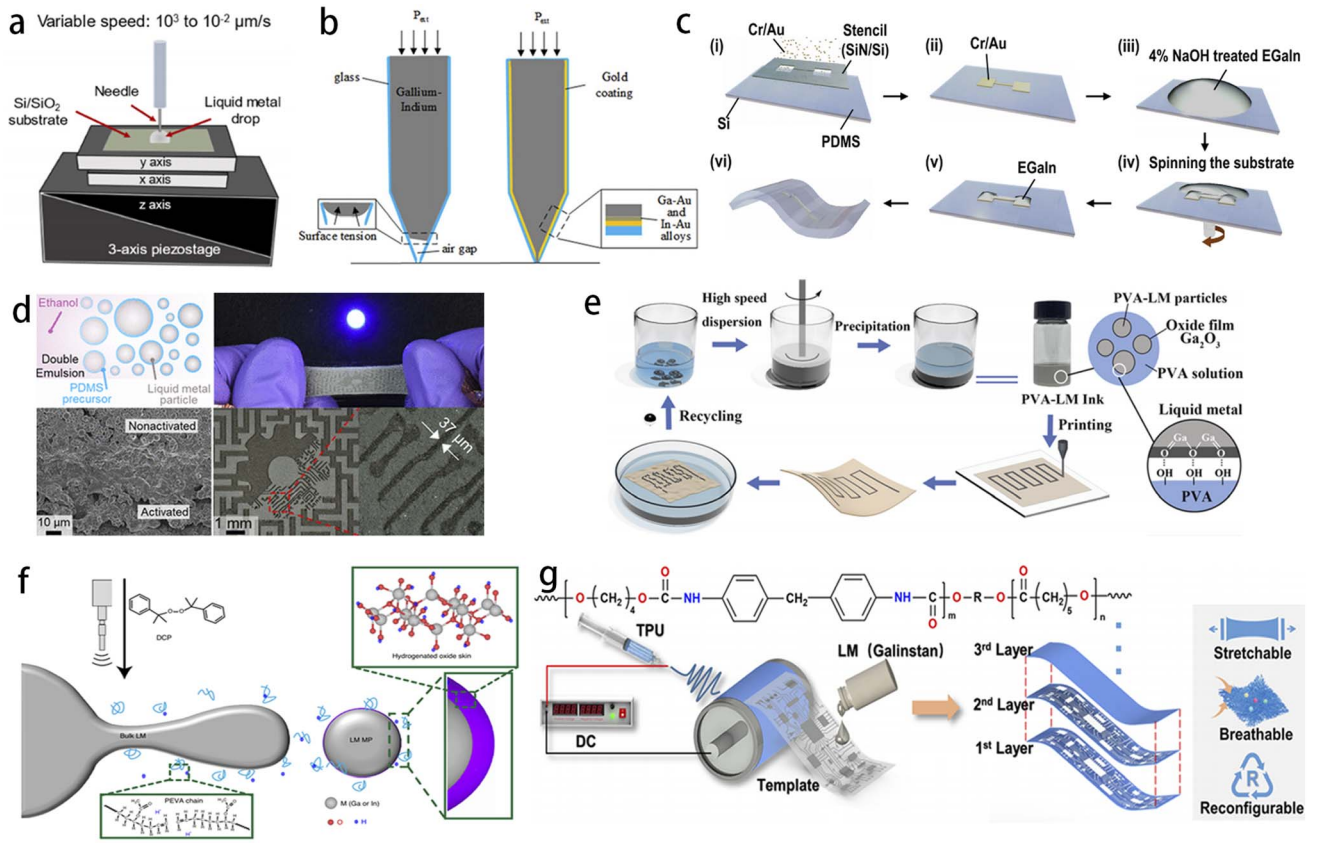

Fig. 1 (a) Schematic diagram of liquid metal nanotip traction device using triaxial piezoelectric stage.[3] (b) Transport of liquid metal in pressurized fountain pen lithography.[5] (c) Stencil printing and centrifugal force-assisted patterning.[4] (d) PVA–LM ink manufacturing, printing, recycling process.[6] (e) Photographs of complex laser-activated maze patterns on PDMS–LM composites.[8] (f) Hydrogen-doped viscoelastic liquid metal particles.[9] (g) Schematic design of flexible electronic systems.[7]

and health monitoring. At present, LM respiratory sensor, liquid metal heartbeat (Fig. 2a),[10] gesture monitor (Fig. 2b),[11] biosensors (Fig. 2d–f), and wrist pulse monitor (Fig. 2c)[12] have been successfully prepared.

Fig. 2a shows the preparation of the LM breath monitor, which has an arched air gap LM magnetoelectric sensor, including LM and magnetic powder materials.[10] It could be driven by exhaled and inhaled breath, and conduct breath monitoring by self-power. It has a high sensitivity of 17.73 kPa^{-1} and a fast response speed. It could be used as a noninvasive, miniaturized, portable respiratory monitoring system to warn of potential health risks. When the human body wears an LM breathing monitoring system for breathing conditions, the sensor could generate an electrical response to diagnose the current breathing status. For chest breathing less than 12 breaths per min, the sensor voltage is less than 2 μV; for normal breathing, 12–20 breaths per min, the sensor voltage is 2–4 μV; and for acute breathing 20–40 breaths per min, the sensor voltage is 4–8 μV. The sensing system provides an early warning signal once the breaths per minute are outside the normal respiratory range.

Fig. 2b is a multilayer LM wire pulse sensor that could be recycled, portable, non-invasive, and scalable. Its printing accuracy is 50 μm, with a tensile capacity of 380%.[11] It could be attached to the knuckle of the hand to achieve accurate gesture detection. This biomedical sensor consists of a transparent wearable electronic skin composed of a 6 × 6 base capacitor array. It enables multitouch monitoring and could be used for patient heartbeat monitoring. It also has the potential to help patients improve their healthcare lives, replace prosthetic devices, track daily movement, and continuous health monitoring.

At the same time, two different types of rigid micropump structures (embedded micro-pump E-bump and anchored micropump A-bump) were used to realize multipurpose pressure-sensitive devices (Fig. 2c).[12] These devices were applied to wireless multi-position wrist pulse monitoring, fingertip pressure sensor gloves, and wireless body sensor–machine interface devices. E-bump and A-bump structures could achieve a susceptible, robust interconnection structure, increasing the average sensor sensitivity to 0.0727 kPa^{-1}, and A-bump reduced the average sensor sensitivity to 0.0004 kPa^{-1}. This sensitivity is improved and controllable. With this liquid metal biomedical sensor, pulse palpation could be performed at three locations on both wrists. These $\Delta R/R_0$ signals could be medically assessed by applying different pressures for three positional pulse measurements, with pulse mode measurements resulting in $\Delta R/R_0$ results of 0.1, 0.2, and 0.3, respectively. Doctors could

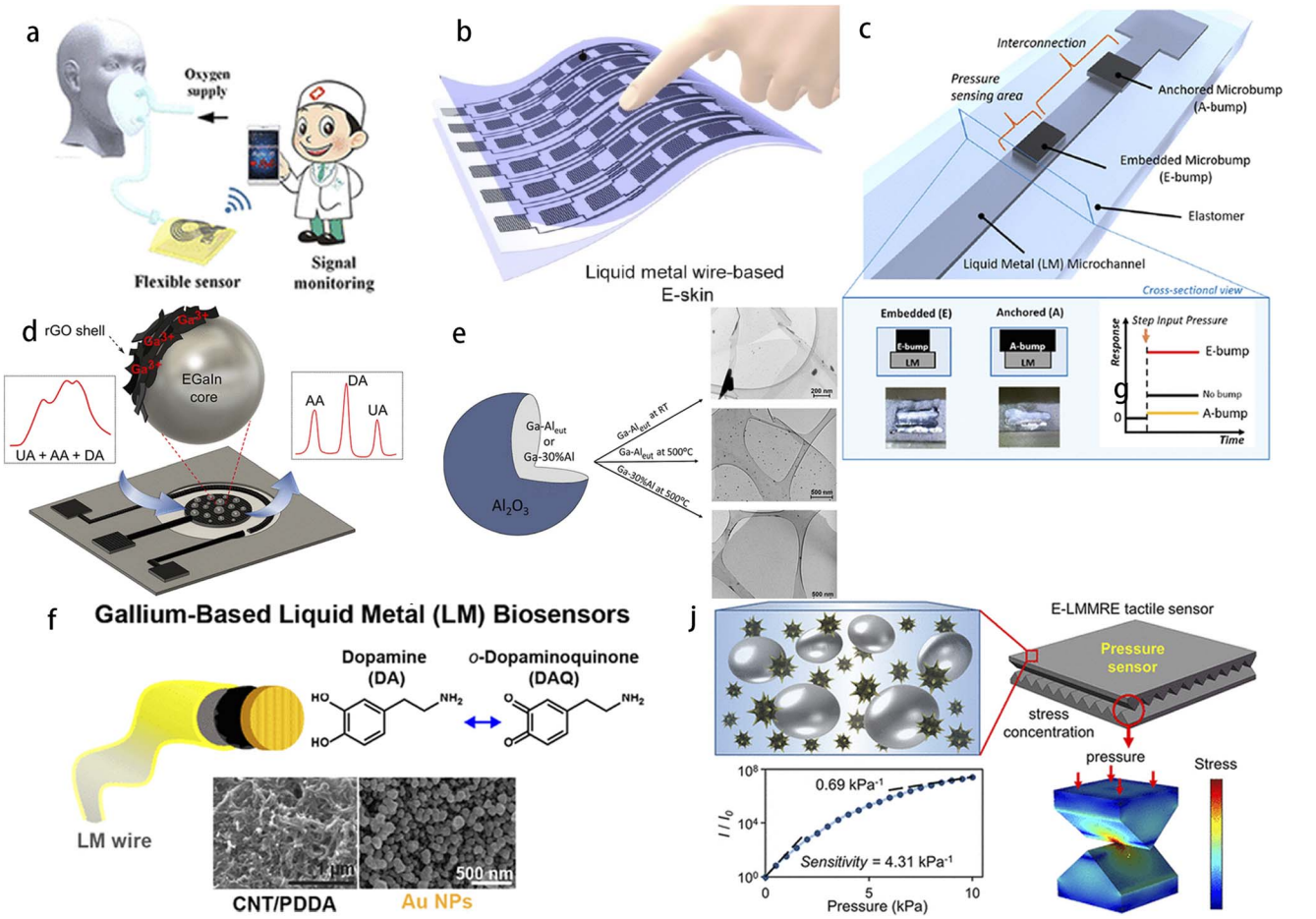

Fig. 2 (a) Schematic diagram of self-powered intelligent respiratory monitoring system.[10] (b) Optical images of digital gestures in China wearing liquid wire-based flexible electronic devices.[11] (c) 3D-printed schematic design of a liquid metal pressure sensor integrating A-bump and E-bump.[12] (d) Reduction of interfacial graphene oxide by liquid metals.[16] (e) Bright-field images of GaAl$_{eut}$ at room temperature, GaAl$_{eut}$ at 500 °C, and Ga-30 at% Al at 500 °C.[14] (f) Multilayer carbon nanotubes/gold nanoparticles composites based on gallium-based liquid metal for electrochemical biosensing.[15] (g) Bio-elastomer based liquid metal filled magnetorheological elastomers.[13]

sense and analyze wrist pulse waveforms with real-time wrist pulse visualization.

Based on a silicone rubber substrate, conductive elastomers filled with spiky nickel particles and LM droplets could be prepared (Fig. 2g).[13] Due to the synaptic structure of the spiky nickel surface, the electrical conductivity of this composite significantly increases by several orders of magnitude under compressive and tensile loads. This composite was extremely sensitive and could be used for pressure sensors. It became an ideal material for tactile perception and mechanical response. By preparing an intelligent heating film with a pyramid structure, the temperature could be adjusted according to the pressure. This flexible pressure sensor has a high sensitivity of 1–3 kPa^{-1}, a high resolution of 2 Pa, and a low detection limit of 2 Pa.

Nano-alumina layer could also be successfully obtained from Ga–Al alloy at room temperature (Fig. 2e). This nano oxide layer obtained from two LM components (including Ga–Al$_{eut}$ and Ga-30 at% Al) was applied to gas sensors.[14] It allows deposition at low temperatures and produces eco-friendly nanomaterials with minimal consumption. The prepared metal oxide nanomaterials have significance for sensors and electronic devices.

An electrochemical sensor is shown in Fig. 2f. Electrochemical deposition deposited the carbon nanotubes on the surface of LM, and then functionalized gold nanoparticles on carbon nanotubes (Fig. 2f).[15] It had electrochemical performance, and showed good dopamine sensing detection performance with a sensitivity of 0.236 ± 0.013 μA μM^{-1} and a LOD of 23.2 nM. It has high-performance electrochemical sensing and biological stability compared with the current dopamine-sensing electrochemical apparatus.

At the same time, there is a strong galvanic interaction between LM and graphene oxide (GO), which could be used to generate RGO monolayers and thick films (Fig. 2d).[16] RGO film of different thickness could be produced on the surface of LM to form LM–rGO–shell structure. In the presence of other biological disturbances, by synthesizing LM–RGO composites on LM droplets for selective biosensing of dopamine, biosensors could also be prepared. One of the body's neuromodulators, dopamine could be monitored using a liquid metal electrochemical

sensor. Differential pulsed voltammetry (DPV) and cyclic voltammetry (CV) changes (30–90 μA) in electrochemical signals could be recorded by exposing bare and liquid metal-modified electrodes to solutions containing dopamine mixtures. The observed peak separation enables low-cost, portable dopamine measurements.

Research progress of liquid metal catalysts

Liquid metals would be further developed in catalysis,[17] catalytic hydrogen production,[18] and catalytic atom transfer of free radicals.[19]

At room temperature, a LM base method is proposed for the catalytically assisted deposition and graphitization of molybdenum dioxide (MoO_2) (Fig. 3h).[20] Introducing molybdate precursors around the eutectic GaIn alloy droplets formed a uniform hydrated molybdenum oxide layer (H_2MoO_3) at the interface. By using this transferred H_2MoO_3 layer, a laser writing technique was developed to selectively convert H_2MoO_3 into crystalline MoO_2, and generate a conductive pattern with plasma characteristics. The obtained method of metal oxide deposition and mapping has been widely used in optoelectronics, sensing, and energy.

Through liquid Ga-assisted chemical vapor deposition to prepare 2P–N heterojunction, vertical GaSe/MoS_2 controlled growth was reported (Fig. 3c).[21] By adjusting the amount of Ga, the growth mode between vertical and transverse could be precisely changed. P–N heterojunction was further studied based on this realized vertical GaSe/MoS_2. Under the illumination condition, the photovoltaic effect of this photosensitive device was significant, which has a large open circuit voltage of 0.61 V and a broadband detection capability of 375–633 nm. It could be further used for autonomous light detection with a high response of 900 mA W^{-1}, and a fast response speed of 5 ms.

Two-dimensional (2D) aluminum hydroxide with high electrostatic polarization was prepared using LM as a reaction platform (Fig. 3g).[22] By changing the synthesis conditions of Ni^{2+} and Co^{2+} ions, the OH bond was used as the adsorption site, and 2D Al/NiCo-LDO layered double oxides nanosheets could be obtained. This developed frame has a good electron beam absorption performance. And this synthesis method has

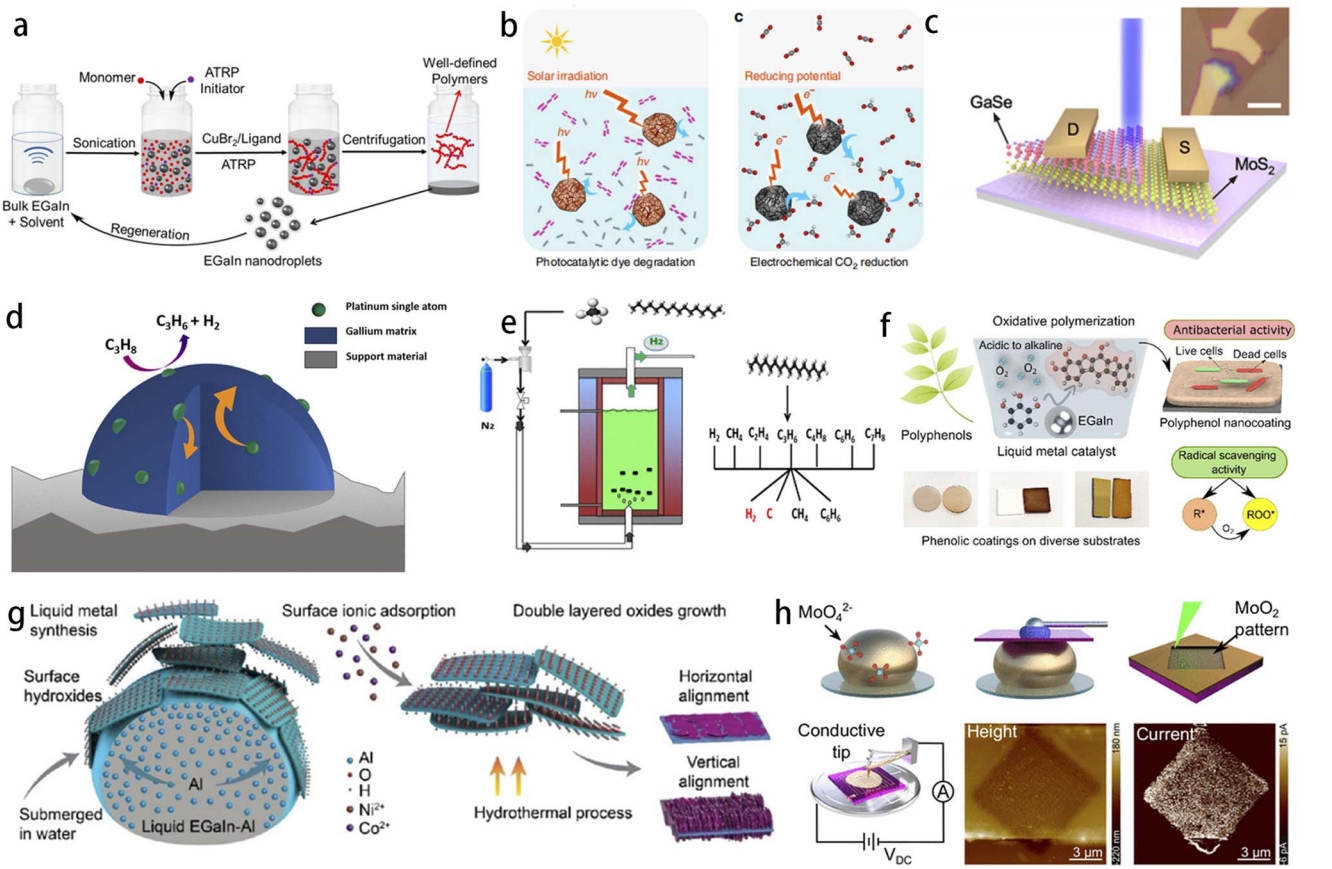

Fig. 3 (a) Liquid metal catalyzes atom transfer radical polymerization.[24] (b) Liquid metal alloys are used to make catalysts in nanometallurgy.[27] (c) Schematic diagram of vertically stacked GaSe/MoS_2 heterostructure devices.[21] (d) Schematic diagram of propane dehydrogenation catalyst.[26] (e) Simplified description of the fuel pyrolysis process in a liquid metal bubble reactor.[25] (f) EGaIn is a heterogeneous catalyst to produce thin phenolic coatings under acidic to alkaline conditions.[23] (g) Liquid metal derived two-dimensional layered bisoxide nanoplates.[21] (h) Liquid metal assisted low-temperature molybdenum dioxide deposition.[19]

broad application prospects in electron beam absorption and electromagnetic protection.

LM was also used as a catalyst to promote the oxidative self-polymerization of natural polyphenols (Fig. 3f).[23] The oxidative polymerization of polyphenols initiated by LM resulted in very high reaction kinetics of the nano-coating. Highly active free radical species were produced, which enabled the rapid oxidation of polyphenols. Moreover, phenolic nano-coatings obtained from acidic pH environments have good antioxidant and antibacterial properties. This method could also be used in industry, food science, and biomedicine.

EGaIn micro/nanodroplets with a high surface area could be applied in atom transfer radical polymerization (ATRP) (Fig. 3a).[24] LM micro/nanodroplets were mixed with a Cu II complex, monomer, and alkyl halide initiator in an N_2 atmosphere. In the presence of LM, ATRP produces well-defined polymers. LM nanodroplets could reduce Cu II complex to Cu I complex, which could be used as an activator of ATRP.

A new method of hydrogen production from complex hydrocarbon fuel pyrolysis is discussed. The methane decomposition process of hydrocarbon fuel in LM bubble reactor could be divided into two stages: the pyrolysis intermediates are simulated based on the functional group dynamics model; the quantities of the main products (CH_4, H_2, Cs, C_6H_6) from secondary pyrolysis of intermediates were simulated using a detailed high-temperature mechanism and approximated by a simplified regression equation (Fig. 3e).[25] The further decomposition of smaller hydrocarbons until they exit the reactor was simulated. The mixed effects of bubble coalescence and bubble rupture were studied in a reactor. The results show that the H/C ratio and cyclic/aromatic content are the main factors affecting the total H_2 conversion.

The chemical cycling of LMs (Bi, In, and Ti) from low calorific value exhaust gases (*e.g.*, blast furnace gas) as effective modifiers for iron-based redox catalysts has been investigated at moderate temperatures (450–650 °C).[18] The bismuth modifier forms a coating layer on the Fe oxide matrix and has better anticoking performance than the Fe oxides supported by $La_{0.8}Sr_{0.2}FeO_3$ and $Ce_{0.9}GD_{0.1}O_2$. In the cyclic redox reaction at 550 °C, the sintering resistance and redox activity of bismuth-modified samples were also improved, and the oxygen capacity was 4 times higher than that of the original Fe_2O_3 (28.9 *vs.* 6.4 wt%). The redox performance of the compound was enhanced effectively. Liquid metal (Bi, In, *etc.*) modified iron oxides could be used as catalysts for low calorific value exhaust gases. Hydrogen could be generated from the fuel by a cyclic redox process.

Narayanan Raman *et al.* investigated the dehydrogenation of propane with Pt-supported catalyzed active LM solution (SCALMS) at Ga (2 at% Pt) in the temperature range of 500–600 °C (Fig. 3d).[26] The catalyst was synthesized on silicon dioxide (SiO_2), alumina (Al_2O_3), and silicon carbide (SiC). The results show that the SiC-based SCALMS catalyst has the highest activity, while the SiO_2-based SCALMS catalyst has most increased stability and the lowest cracking tendency at a higher temperature. At 600 °C, the selectivity of SiO_2-based catalyst to propylene remained above 93%. The coke content was analyzed by temperature-programmed oxidation (TPO) and Raman spectroscopy. The coke content of SCALMS supported by SiC and SiO_2 had almost no coking phenomenon, while that of SCALMS supported by Al_2O_3 had an obvious coking phenomenon.

During the solidification process of the Bi–Ga alloy system, highly ordered nanopatterns appear preferentially on the surface of the alloy. Various transition, hybridization, crystal defect patterns, and lamellar and rodlike structures, have been observed (Fig. 3b).[27] The effects of Bi and Ga_2O_3 layers on the surface solidification process were studied by combining experimental and molecular dynamics simulations. And the formation mechanism of heterogeneous nucleation mode was found. The dynamic heterogeneous nucleation mode was found. The dynamic characteristics of this phenomenon under different solidification conditions and alloy systems were demonstrated. Bi–Sn nano-alloy transformed binary oxide $Bi_2Sn_2O_7$ could be applied to photocatalytic Congo dye degradation. Its degradation rate constant (slope of the $\ln(c_0/c_t) - t$ curves) could reach 80%.

Research progress of liquid metal composites

Flexible electronic devices have penetrated every industry in human life, for example consumer electronics, automotive, and medical. They require stretchable conductive composite materials to provide better performance. Conductive composites have been traditionally prepared by adding conductive inorganic fillers into flexible polymers. Due to limited deformation, low electrical conductivity, and poor machinability, the performance of conductive composites could not meet the requirement of today's demanding equipment. Currently, LM could be used in composite materials to prepare row memory composite materials and another flexible composite.[28–32]

LM–TPE composite wires were prepared by electrospinning porous thermoplastic elastomer microfibers and coated with LM (Fig. 4k).[33] For packaging, another layer of electrostatic spinning TPE ultrafine fiber was deposited on this steel wire. The porous structure of electrostatic spinning fibers could significantly improve the tensile property and electrical stability of LM–TPE wires. A stretchable conductor was developed by simply spraying or printing LM on an elastic fiber mat of electrospinning. In addition, it has good biocompatibility and intelligent adaptability. Compared to these wires using nonporous TPE as a matrix, the breaking strain of LM–TPE wires increased. Under the tensile pressure of 1900%, the increase in resistance of the wires could be controlled by less than 12 times, which is much more stable than other one-dimensional LM-based elastic conductors.

A highly deformable eutectic LM embedded in natural rubber (NR) structure was prepared (Fig. 4b),[34] using industrially feasible solid-state mixing and vulcanization. The standard vulcanization method allowed us to break and disperse LM into submicron droplets in crosslinked NR. This composite material has a six-fold increase in tear resistance, a four-fold decrease in

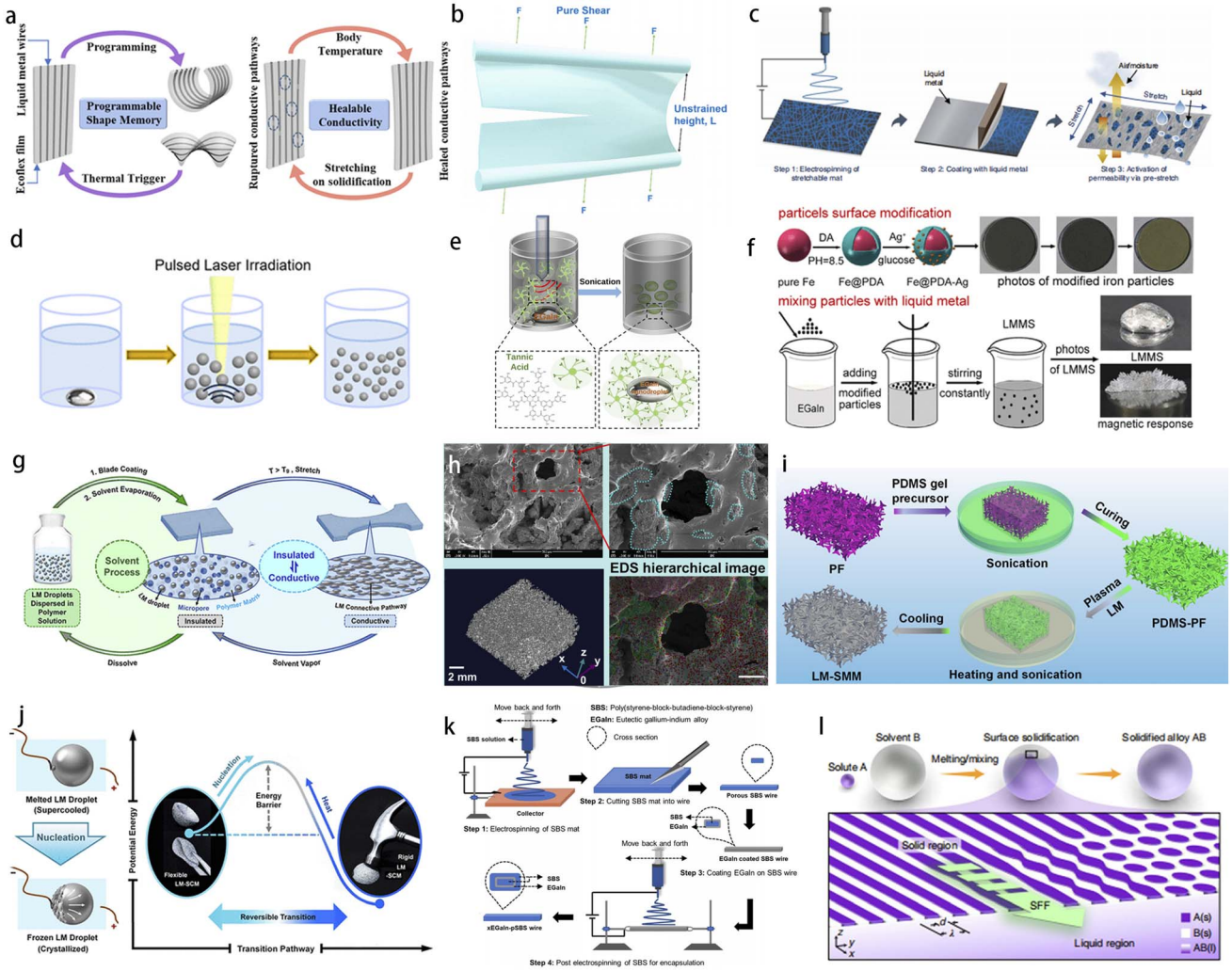

Fig. 4 (a) Soft stretchable liquid metal composite with shape memory and healing conductivity.[41] (b) Super stretched liquid metal embedded natural rubber composite.[34] (c) Schematic diagram of a typical manufacturing process for a liquid metal fiber pad.[51] (d) Anisotropic conductive adhesive for liquid metal nanodroplet.[38] (e) Conductive hydrogel adhesive containing liquid metal.[35] (f) Liquid metal maglev with rheological, magnetic, electric, and thermal strengthening.[40] (g) Solvent machinability and insulator-to-conductor reversible transition of microporous liquid metal embedded in polymer films.[37] (h) Schematic diagram of "Taiji" of liquid metal foam film.[39] (i) Highly conductive liquid metal-based shape memory material.[42] (j) Stiffness changes of liquid metal composites driven by electricity.[36] (k) Manufacturing scheme for super stretchable xEGaIn-pSBS line. (l) Schematic diagram of surface solidification process.[52]

crack growth, and significant improvement in mechanical (up to 650% strain at failure) and elastic properties. The composites' thermal conductivity and dielectric properties were also improved, providing a simple and extensible way to develop LM-embedded soft elastomer composites.

By mixing LM nanodroplets coated with tannic acid with catechol functionalized chitosan (PCHI-C), cholesterol, aldehyde-modified glucan (PDEX-ALD-CH), and PEDOT:Hep, a complex polymer network was synthesized (Fig. 4e).[35] Biomimetic conductive self-assembly hydrogel was also synthesized by polysaccharide, conductive biopolymer, and LM nanodroplet. The structure and concentration of each intermediate could be varied, resulting in a modular system with adjustable mechanical, physical, and biochemical properties. After polymerization and synthesis, it could combine materials with different properties to generate a matrix with high adhesion strength, enhanced electrical conductivity, good cytocompatibility *in vitro*, and high biocompatibility *in vivo*. This reversible network has properties of self-healing and shear thinning. The high biocompatibility was demonstrated in immunoactivity mice by allowing 3D printing and minimally invasive injection *in vivo* experiments.

Adding LM Ga into flexible and porous polymer matrix (porosity 78.93%) could prepared LM composite with varying stiffness (Fig. 4j).[36] This composite has high conductivity and reversible stiffness transformation could be easily triggered by a small voltage of 5 V in the electrolyte. When the external voltage was removed, the stiffness remained constant. This LM-based stiffness variable material showed a 1000-fold modulus difference (65–79 MPa). This composite material could be

successfully used to construct intelligent valves, mechanical claws, and other robots in the marine environment.

Through the solvent evaporation-induced microporous method, LM was fused into a matrix of microporous polymer (ABS/PMMA/PMMA-*co*-BMA), and a stretchable microporous LM embedded polymer film was prepared (Fig. 4g).[37] This composite film was insulating but became conductive during the stretching. Under the action of organic vapor, this microporous LM-embedded polymer film exhibits reversible insulation–conductor transition (8.3 Ω). After 50 solvent exposure tensile strain cycles, the change of resistance value was ignored, and it has excellent stability. This composite membrane could be used in hazard sensors, solvent leakage alarm devices, and protective switches, which has incredible potential in sensor applications. By combining laser irradiation and ultrasound, a series of core–shell eutectic LM nanodroplets with different diameters were successfully synthesized (Fig. 4d).[38] Due to their high conductivity and good fluidity, these LM nanodroplets were used as soft conductive fillers to prepare anisotropic conductive adhesives (ACAs). When used for the interconnection of tiny electronic circuits, these prepared ACAs have good anisotropic conductivity. It could maintain highly durable anisotropic electrical properties in flexible package devices, even in bending or torsional operation modes.

By introducing the thermal decomposition of bicarbonate, LM foams could be designed with the help of environmentally friendly foaming agents (Fig. 4h).[39] The foaming agent ($NaHCO_3$) was uniformly distributed in LM. Then the foaming process was based on the thermal decomposition of $NaHCO_3$ on a heating platform. It has a porous structure, controllable adjustment, rich interface, conductivity, adjustable stiffness, and other excellent performance. This LM foam has a hydrogen evolution in neutral deionized water, and it could also produce high-performance compact foam in an air battery. The prepared adjustable four-dimensional LM foam material has excellent electromagnetic shielding performance.

Using shell core structure Fe@PDA–Ag as particle and LM as the base, LM-based maglev liquid could be prepared, which has good electrical, magnetic, and thermal properties[40] (Fig. 4f). By introducing polydopamine (PDA) *in situ* reduction, the silver shell on the surface of iron particles was fixed, which could prevent the alloying of iron particles with LM, and improve the conductivity and thermal conductivity of the alloy. This LM material could keep its magnetism unchanged during the 60 days of the test. Compared with the mixture of iron particles and LM, the maximum conductivity (2.41×10^6 S m^{-1}) and thermal conductivity (48.95 W m^{-1} K^{-1}) of the LM base magnetic suspension were increased by at least 13.69% and nearly 4 times, respectively. This LM-based magnetic suspension could be used in thermal interface materials, and magnetic manipulation to write and draw patterns.

Shape memory composites could preserve deformed shapes and recover when subjected to specific external stimuli (Fig. 4a).[41] Because LM Ga could control the geometry of the packing, it could be applied to elastomer films containing microchannels and create metal conductive circuits. By integrating LM, polydimethylsiloxane (PDMS), and polyurethane foam, LM-based shape memory material (LM-SMM) was synthesized (Fig. 4i).[42] The flexibility of PDMS ensures good shape recovery performance. The switchable construction and excellent electrical conductivity make the LM-SMM suitable for ultra-sensitive fire alarm responses. This performance enables the LM-SMM to achieve the lowest fire alarm temperature in a short response time, which has broad application prospects in the safe storage of flammable materials.

Research progress of liquid metal driving machine

Micro/nanomotors have made great progress in driving power and precise maneuvering. Ga/In-based LM alloy has good biocompatibility and low biotoxicity;[43] it is the ideal material to solve these problems. Soft crawling robots have potential applications in monitoring, rescue, and detection in complex environments. Most existing soft crawling robots are either driven by passively induced friction asymmetries or could only move on specially designed surfaces. As a result, robots often lack an ability to move in two dimensions, or in any direction of unpredictable environments. In the field of LM drive, new LM micro motor,[44] LM intelligent foot,[45] crawling robot,[46] and LM nano robot[47] have been prepared.

As shown in Fig. 5a, Ga, In, and Sn were dispersed into micro-nano particles by ultrasound, and then metal (Pt, Au, Ag) and nonmetal (SiO_2) were sputtered on LM microspheres.[44] An alkaline-driven LM micro-motor (100 nm to 20 μm) was prepared, which could move in an alkaline solution. The driving mechanism is divided into two kinds: (1) self-electrophoresis: when the sputtering material was metal, there was a current between met-al and LM; (2) self-diffusion electrophoresis: when the sputtering material was non-metallic, there was no current between non-metallic and LM. The driving speed of self-electrophoresis was much faster than that of self-diffusion electrophoresis. The micromotors of LM expand fuel options and could be adapted to different biochemical applications.

The LM intelligent feet were prepared, which could be used for active control of crawling robots (Fig. 5b).[45] This LM brilliant foot consisted of two LM droplets inside a 3D printing stand, and controlled by copper wire. The body was made of elastic composite material, with a shape memory alloy spring embedded in the center. The shape memory alloy spring was encapsulated in a composite with a silicone matrix and nickel particles to enhance heat dissipation. When the LM smart foot was immersed in the electrolyte, friction was electrically controlled. The bidirectional and climbing movement of the robot on various substrates and smooth surface was explored, which display the crawling robot's ability, and achieve multi-function drive prismatic climbing.

A LM nanorobot driven by urease was also proposed. Through photothermal and chemotherapy effects, when it was exposed to near-infrared light, it would deform and achieve synergistic and antibacterial treatment (Fig. 5e).[46] The dual-mode ultrasonic and photoacoustic properties of LM nanoparticles could be used to monitor the active movement of

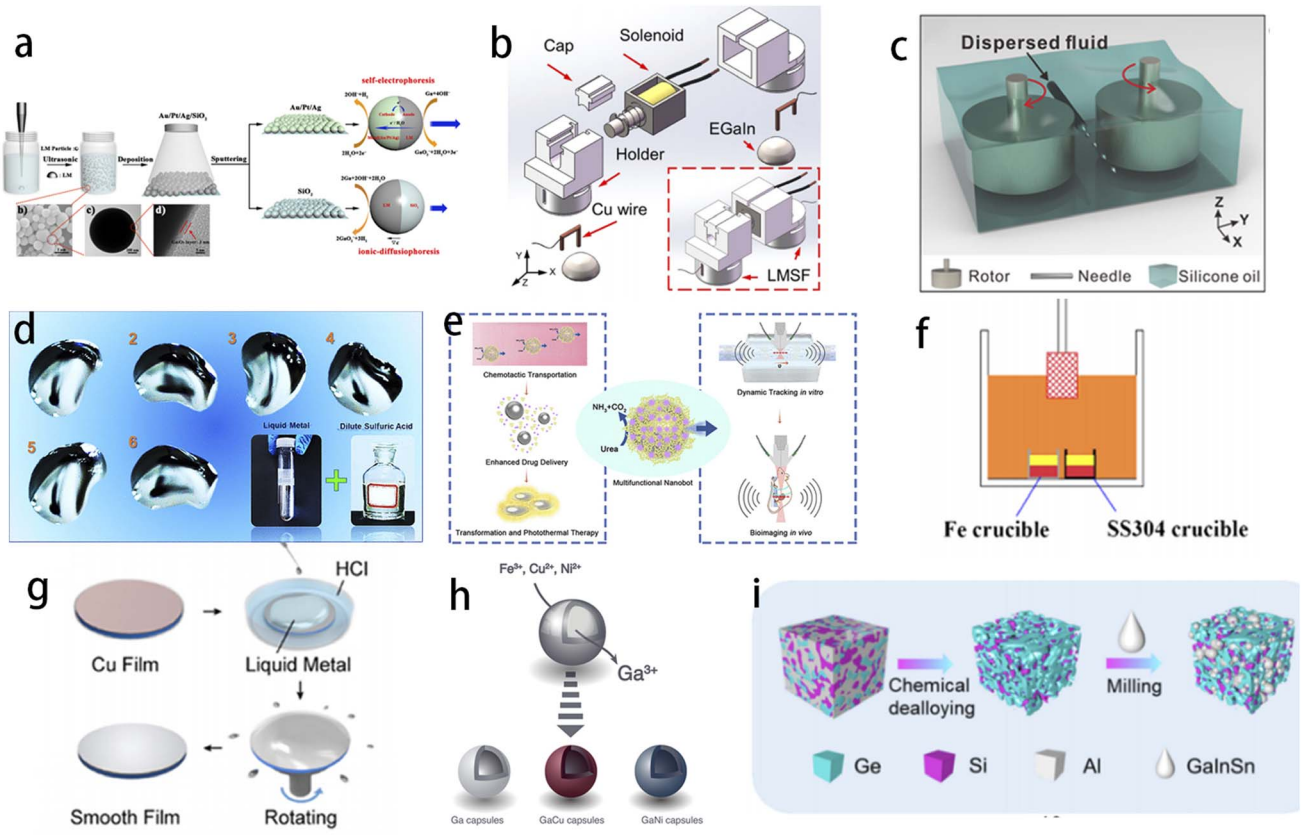

Fig. 5 (a) GaInSn LM Janus micro motor production and motion principal diagram.[44] (b) Schematic of a miniature electromagnetic drive with two liquid-metal smart feet.[45] (c) Schematic diagram of microfluidic strategy rotary flow shear process.[48] (d) Under appropriate conditions, droplets could spontaneously and periodically rotate with a fixed shape like a comma.[47] (e) Schematic diagram of LPCU nanorobot.[46] (f) Complete discharge state of Sb–Sn alloy after electrostatic corrosion. (g) Schematic diagram of the process for manufacturing smooth and uniform liquid metal films as reflective electrodes.[50] (h) Schematic diagram of preparation of porous germanium silicon liquid metal.[53] (i) Schematic diagram of hollow gallium particles and their alloys with transition metals.[49]

a robot in a microfluidic vascular model. It also provides a feasible tool for preclinical studies and clinical trials of image-guided therapy.

By using an acid droplet, the spontaneous and stable rotation of LM droplet was realized. When acid droplets deposit on LM surfaces, they could move spontaneously (Fig. 5d).[47] This phenomenon results from the fluctuation of the droplet boundary, and the movement of bubbles produced by the chemical reaction of the acid and LM. This finding may improve understanding of the transformation of physical systems under the influence of chemical reactions, and provide new avenues for the design of potential micro-nano devices.

Due to the multifunction and structural advantages, non-spherical LM particles (NLMs) show great potential in various applications. A simple microfluidic strategy called rotary flow shearing was proposed to produce efficient, controllable, and template-free shaped NLMs (Fig. 5c).[48] In the carrier fluid, two counterrotating rotors provide high-speed viscous shear flows, that induce continuous clipping of LM from a capillary in front of a slit. Real-time oxidation enables rapid solidification of the extrusion neck and LM surfaces, resulting in many NLMs. Rotary flow shearing makes the NLMs shape adjustable, especially for high-viscosity working materials. Under the action of the applied electric field, the collected NLMs exhibit unique electrostatic response properties, including translation, rotation, reciprocation, and alignment.

Research progress of liquid metal electrode

LM was used to modify the nano-porous SiGe. Al was selectively removed from $Ge_8Si_{12}Al_{80}$ alloy by chemical etching in an acidic solution, and the nanoporous structure was formed (Fig. 5i).[49] LM was stirred and mixed with the SiGe, and the LM particles were successfully embedded into the SiGe hole structure to create a LM base electrode. This LM composite anode improved the cycling stability of nano alloy anode and showed high reversible lithium storage performance and self-healing properties. After 300 cycles at room temperature, the capacity is 1200 mA h g^{-1}; after 100 cycles at −20 °C, the capacity is 746.7 mA h g^{-1}.

By depositing smooth and uniform LM films on a large and elastic substrate, stretchable reflective electrodes could be prepared (Fig. 5g).[50] Thermal evaporation deposited Cu films on the substrate, and the LM was diffused onto the metalized

substrate. The thickness of the LM film (1.6 μm) was controlled by high-speed rotation. This electrode could maintain good electrical conductivity and optical reflectance under a large deformation. The prepared electrode has a low chip resistance (0.15 Ω Sq.$^{-1}$), high optical reflectance (95% at 550 nm), and ultra-high deformation (500%), which could withstand repeated tensile deformation. This electrode could be used in various optoelectronic devices, such as stretchable displays, intelligent wearables, and deformable solar cells.

Conclusions

This paper reviews the applications and principles of LMs in different fields in the past year. First, in the area of sensing applications, LM is used for respiratory monitoring, biomedical sensing, electrochemical sensing, *etc.* The device has high sensitivity, dramatically reduces error, improves biological stability and electrochemical performance, and plays an essential role in monitoring human health. The potential biosensing application of LM devices is opened through the electrochemical deposition of nanomaterials on gallium alloy, which has excellent application in intelligent artificial skin and soft robot fields.

Secondly, in the field of catalysis, LM is used in photocatalysis, catalytic hydrogen production, catalytic atom transfer radical, electrocatalysis, and so on. The application of the LM catalyst will continue to develop in the future, and its catalytic performance will continue to improve. LM with a low melting point, large contact area, and good solubility could be used as a popular material for multifunctional catalysts. LM single/multi-catalyst, multiphase catalyst, multifunction, green, and high efficiency are the critical development direction in the future.

In the field of printing, this paper summarizes laser printing, template printing, and the development of new liquid metal ink. The research of low melting point metal melt deposition printing, liquid phase printing, compound printing, suspension printing, microcontact printing has also made progress. Through template printing, flexible circuits, resistors, capacitors, inductors, and multilayer reconfigurable composite devices with good stretchability, permeability, and stability could be prepared by parameterization. Recyclable LM ink stability, and high sensitivity in alkaline conditions could be recycled and reduce environmental pollution.

In the field of composites, LM shape memory composites with healing conductivity have been used in flexible electronics and soft robotics. LM phenolic nanocoating composites have good oxidation resistance and antibacterial properties, which are widely used in industry, food science, and biomedical fields. Electrostatic spinning elastic fiber pad with strong tensile performance, spraying/printing LM could be made into flexible electronic products. The magnetic, electric, and thermal properties of LM-based maglev, LM-based shape memory material, and LM-based stretchable conductor have been greatly improved. These LM composites were widely used in magnetic operation, optoelectronics, sensing, and energy fields.

In the field of driving, the research on the properties of LM crawling robot drive, nano LM drive, *etc.* It also has implications for potential monitoring, rescue, detection applications, development of advanced LM soft robot systems.

Future challenges, potential advances, and emerging trends in liquid metals in various fields were discussed as follows: in terms of sensing, liquid metal in the future is expected to prepare a lot of ultra-thin, small, highly flexible, susceptible human wearable sensor parts, which are expected to carry out the human body's multi-physiological parameter measurements and extensive data health monitoring. These liquid metal sensor devices are expected to provide real-time and accurate indications of the body's physical condition in the medical field. In terms of catalysis, the applications of liquid metal catalysts will continue to develop in the future, with catalysts that may be applied to a broader range of organocatalytic reactions, most of which have not yet been attempted, such as hydrocarbon addition or dehydrogenation, and chain-breakage responses, with improving catalytic performance. In the printing field, it is expected to develop more liquid metal composite inks with better conductivity, adhesion, and printability and to mix liquid metals with more different polymer materials to produce more composite inks. Additional liquid metal 3D printing technologies could be developed in the future. In composites, more various polymer materials can also be matched with liquid metals through modification methods to form more functional composites. In robotics, liquid metal could be combined with materials such as liquid crystals to prepare more foldable micro-driving machines.

This paper comprehensively summarizes the application of LM in different practical fields, which helps understand the development trend and direction of LM materials, and lays a foundation for the development of metal materials in the next step.

Author contributions

The author's contributions are as follows: Shuting Liang oversaw the whole trial, and wrote the manuscript; Jie Yang wrote part of the manuscript; Fengjiao Li, Shunbi Xie, Na Song, and Liang Hu assisted with sampling and laboratory analyses. All authors have given approval to the final version of the manuscript.

Conflicts of interest

There are no conflicts to declare.

Acknowledgements

This research was financially supported by Scientific Research Fund of Chongqing Municipal Education Commission (KJQN202201306), Major Cultivation Program of Chongqing University of Arts and Sciences (P2022HH06), Natural Science Foundation of Yongchuan District (2023yc-jckx20067), Key Laboratory of Intelligent Textile and Flexible Interconnection of Zhejiang Province (No. YB03), and Guangdong Basic and

Applied Basic Research Foundation (No. 2021A1515010150). The authors express gratefulness for helpful comments from reviewer and editor to improve this manuscript.

References

1 S. Chen, Z. L. Cui, H. Z. Wang, X. L. Wang and J. Liu, Liquid metal flexible electronics: past, present, and future, *Applied Physics Reviews*, 2023, **10**, 021308.

2 S. T. Liang and X. Y. Chen, Laser-engraved liquid metal circuit for wearable electronics, *Bioengineering*, 2022, **9**, 59.

3 M. A. Francois, J. L. Han, J. B. Tang, M. Salma, S. X. Cai, J. M. Tang, A. Roozbeh, C. Franco, M. Maedehsadat, C. C. Zhang, W. J. Xie, M. Mohannad, A. R. Md, B. G. Mohammad and K. Z. Kourosh, Nanotip Formation from Liquid Metals for Soft Electronic Junctions, *ACS Appl. Mater. Interfaces*, 2021, **13**, 43247–43257.

4 Y. C. Sun, G. Boero and B. Jurgen, Stretchable Conductors Fabricated by Stencil Lithography and Centrifugal Force-Assisted Patterning of Liquid Metal, *ACS Appl. Electron. Mater.*, 2021, **3**, 5423–5432.

5 G. I. Livshits, J. Bao, L. Sakamoto, *et al.*, Sacrificial gold coating enhances transport of liquid metal in pressurized fountain pen lithography, *Sci. Rep.*, 2021, **11**, 4670.

6 S. L. Liu, S. Y. Kim, K. E. Henry, D. S. Shah and R. K. Bottiglio, Printed and Laser-Activated Liquid Metal-Elastomer Conductors Enabled by Ethanol/PDMS/Liquid Metal Double Emulsions, *ACS Appl. Mater. Interfaces*, 2021, **13**, 28729–28736.

7 J. Y. Xu, H. D. Guo, H. Y. Ding, Q. Wang, Z. Q. Tang, Z. J. Li and G. X. Sun, Printable and Recyclable Conductive Ink Based on a Liquid Metal with Excellent Surface Wettability for Flexible Electronics, *ACS Appl. Mater. Interfaces*, 2021, **13**, 7443–7452.

8 M. Wang, C. Ma, P. C. Uzabakiriho, X. Chen, Z. R. Chen, Y. Cheng, Z. R. Wang and G. Zhao, Stencil Printing of Liquid Metal upon Electrospun Nanofibers Enables High Performance Flexible Electronics, *ACS Nano*, 2021, **15**, 19364–19376.

9 V. Selvaraj, J. Woosun, B. S. Jae, H. B. Wang, K. Minsik, T. Kaliannan, K. Junghyeok, P. Gyeongbae, L. Gilwoon, S. Wonjeong, Y. Insang, E. K. Mehmet, G. Anupam, B. Lucia, S. Aloysius and J. Unyong, Hydrogen-doped viscoplastic liquid metal microparticles for stretchable printed metal lines, *Nat. Mater.*, 2021, **20**, 533–540.

10 X. Zhang, J. W. Ai, R. P. Zou and B. Su, Compressible and Stretchable Magnetoelectric Sensors Based on Liquid Metals for Highly Sensitive, Self-Powered Respiratory Monitoring, *ACS Appl. Mater. Interfaces*, 2021, **13**, 15727–15737.

11 G. Y. Li, F. K. Sun, H. S. Chen, Y. Jin, A. B. Zhang and J. K. Du, High-Efficiency Large-Area Printed Multilayer Liquid Metal Wires for Stretchable Biomedical Sensors with Recyclability, *ACS Appl. Mater. Interfaces*, 2021, **13**, 56961–56971.

12 O. Gul, K. Y. Kim, J. M. Gu, J. G. Choi, D. O. H. Dionisio, J. S. Ahn and I. K. Park, Sensitivity-Controllable Liquid-Metal-Based Pressure Sensor for Wearable Applications, *ACS Appl. Electron. Mater.*, 2021, **3**, 4027–4036.

13 G. L. Yun, S. Y. Tang, H. D. Lu, T. Cole, S. S. Sun, J. Shu, J. H. Zheng, Q. T. Zhang, S. W. Zhang, M. D. Dickey and W. H. Li, Liquid Metal Hybrid Composites with High-Sensitivity and Large Dynamic Range Enabled by Micro- and Macrostructure Engineering, *ACS Appl. Polym. Mater.*, 2021, **3**, 5302–5315.

14 D. Alexandra, W. Anna, M. M. Marzec, P. Ozga and T. Gancarz, Nanometric Al_2O_3 Layers Obtained from Liquid Metals: Implications for Sensing Devices, *ACS Appl. Nano Mater.*, 2022, **5**(1), 430–437.

15 T. W. Lim and H. N. Zhang, Multilayer Carbon Nanotube/Gold Nanoparticle Composites on Gallium-Based Liquid Metals for Electrochemical Biosensing, *ACS Appl. Nano Mater.*, 2021, **4**, 12690–12701.

16 M. Baharfar, M. Mayyas, M. Rahbar, F. M. Allioux, J. B. Tang, Y. F. Wang, Z. B. Cao, F. Centurion, R. H. Jalili, G. Z. Liu and K. K. Zadeh, Exploring Interfacial Graphene Oxide Reduction by Liquid Metals: Application in Selective Biosensing, *ACS Nano*, 2021, **15**, 19661–19671.

17 H. W. Stephan, J. S. Florian and X. C. Zhou, Critical Review on the Physical Properties of Gallium-Based Liquid Metals and Selected Pathways for Their Alteration, *J. Phys. Chem. C*, 2021, **125**, 20113–20142.

18 I. Wang, Y. F. Gao, X. J. Wang, R. X. Cai, C. C. Chung, I. Sherafghan, W. Wang and F. X. Li, Liquid Metal Shell as an Effective Iron Oxide Modifier for RedoxBased Hydrogen Production at Intermediate Temperatures, *ACS Catal.*, 2021, **11**, 10228–10238.

19 M. Q. Zeng, L. Y. Li, X. H. Zhu and L. Fu, A Liquid Metal Reaction System for Advanced Material Manufacturing, *Acc. Mater. Res.*, 2021, **2**(8), 669–680.

20 Y. F. Wang, M. Mayyas, J. Yang, B. G. Mohammad, J. B. Tang, M. Maedehsadat, J. L. Han, A. Mostak, B. Mahroo, G. Z. Mao, Y. Yao, E. Dorna, C. David and K. Z. Kourosh, Liquid-Metal-Assisted Deposition and Patterning of Molybdenum Dioxide at Low Temperature, *ACS Appl. Mater. Interfaces*, 2021, **13**, 53181–53193.

21 Z. X. Zou, J. W. Liang, X. H. Zhang, C. Ma, P. Xu, X. Yang, X. Zhou, S. Zeng, X. X. Sun, C. G. Zhu, D. L. Liang, X. J. Zhuang, D. Li and A. L. Pan, Liquid-Metal-Assisted Growth of Vertical GaSe/MoS_2 p–n Hetero-junctions for Sensitive Self-Driven Photodetectors, *ACS Nano*, 2021, **15**, 10039–10047.

22 X. F. Zhang, L. L. Xu, J. T. Zhou, W. J. Zheng, J. Han, Z. Karma, K. L. Gang, J. Liu and Z. Ali, Liquid Metal-Derived Two-Dimensional Layered Double Oxide Nanoplatelet-Based Coatings for Electromagnetic Wave Absorption, *ACS Appl. Nano Mater.*, 2021, **4**, 9200–9212.

23 C. Franco, N. Z. Rashin, F. Nieves, T. Mohammad, M. Salma, A. Roozbeh, M. Mohannad, M. A. Francois, J. B. Tang, A. D. William, B. Cyrille, M. D. Dickey, K. Z. Kourosh and M. A. Rahim, Liquid Metal-Triggered Assembly of Phenolic Nanocoatings with Antioxidant and Antibacterial Properties, *ACS Appl. Nano Mater.*, 2021, **4**, 2987–2998.

24 Q. B. Wei, M. K. Sun, F. Lorandi, R. G. Yin, J. J. Yan, T. Liu, K. Tomasz and M. Krzysztof, Cu-Catalyzed Atom Transfer Radical Polymerization in the Presence of Liquid Metal Micro/Nanodroplets, *Macromolecules*, 2021, **54**, 1631–1638.

25 A. Fabiyan, A. Faseeh, K. Muralikrishna, X. Y. Zhang and S. M. Sarathy, Hydrogen Evolution from Hydrocarbon Pyrolysis in a Simulated Liquid Metal Bubble Reactor, *Energy Fuels*, 2021, **35**, 14597–14609.

26 N. Y. Raman, M. Wolf, M. Heller, H. W. Nina, T. Nicola, H. Marco, F. Peter and W. Peter, GaPt Supported Catalytically Active Liquid Metal Solution Catalysis for Propane Dehydrogenation–Support Influence and Coking Studies, *ACS Catal.*, 2021, **11**, 13423–13433.

27 J. Tang, R. Daiyan, M. B. Ghasemian, *et al.*, Advantages of eutectic alloys for creating catalysts in the realm of nanotechnology-enabled metallurgy, *Nat. Commun.*, 2019, **10**, 4645.

28 S. Takashi, Y. Kento, H. Michinao and I. Eiji, Method to Reduce the Contact Resistivity between Galinstan and a Copper Electrode for Electrical Connection in Flexible Devices, *ACS Appl. Mater. Interfaces*, 2021, **13**, 18247–18254.

29 M. Biao, X. Chengtao, C. Lishan, Z. Chao and L. Hong, Magnetic Printing of Liquid Metal for Perceptive Soft Actuators with Embodied Intelligence, *ACS Appl. Mater. Interfaces*, 2021, **13**, 5574–5582.

30 S. Chen, H. Z. Wang, R. Q. Zhao, W. Rao and J. Liu, Liquid Metal Composites, *Matter*, 2020, **2**, 1446–1480.

31 S. T. Liang and J. Li, Flexible Liquid Metal Composite Fiber and Its Intelligent Textiles, *ACS Omega*, 2022, **7**, 12891–12899.

32 S. T. Liang, C. W. Wang, F. J. Li and G. Song, Supported Cu/W/Mo/Ni—Liquid Metal Catalyst with Core-Shell Structure for Photocatalytic Degradation, *Catalysts*, 2021, **11**, 1419.

33 N. J. Zhou, B. F. Jiang, X. He, Y. S. Li, Z. J. Ma, H. Zhang and M. J. A. Zhang, Super Stretchable and Ultrastable Liquid Metal–Elastomer Wire for Soft Electronic Devices, *ACS Appl. Mater. Interfaces*, 2021, **13**, 19254–19262.

34 S. B. Shib, M. Subhradeep, A. Injamamul, K. L. Rama, K. G. Anik, K. Yang, K. Jayant, F. Petr, F. Andreas, H. Gert and D. Amit, Designing Supertough and Ultrastretchable Liquid Metal Embedded Natural Rubber Composites for Soft-Matter Engineering, *ACS Appl. Mater. Interfaces*, 2021, **13**, 15610–15620.

35 Y. Xu, R. Rothe, D. Voigt, *et al.*, Convergent synthesis of diversified reversible network leads to liquid metal-containing conductive hydrogel adhesives, *Nat. Commun.*, 2021, **12**, 2407.

36 Y. M. Xin, T. L. Gao, J. Xu, J. Y. Zhang and D. F. Wu, Transient Electrically Driven Stiffness-Changing Materials from Liquid Metal Polymer Composites, *ACS Appl. Mater. Interfaces*, 2021, **13**, 50392–50400.

37 Y. M. Xin, J. Y. Lan, J. Xu, D. F. Wu and J. Y. Zhang, Vapor-Mediated Stretchable and Reversible Conductors from Microporous Liquid Metal Polymers, *ACS Appl. Mater. Interfaces*, 2021, **13**, 19351–19359.

38 G. Y. Bo, H. W. Yu, L. Ren, N. Y. Cheng, H. F. Feng, X. Xu, S. X. Dou, H. Q. Wang and Y. Du, Gallium–Indium–Tin Liquid Metal Nanodroplet-Based Anisotropic Conductive Adhesives for Flexible Integrated Electronics, *ACS Appl. Nano Mater.*, 2021, **4**, 550–557.

39 J. Y. Gao, J. Ye, S. Chen, J. H. Gong, Q. Wang and J. Liu, Liquid Metal Foaming via Decomposition Agents, *ACS Appl. Mater. Interfaces*, 2021, **13**, 17093–17103.

40 Y. Y. Lu, Z. X. Che, F. Y. Sun, S. Chen, H. Zhou, P. J. Zhang, Y. Yu, L. Sheng and J. Liu, Mussel-Inspired Multifunctional Integrated Liquid Metal-Based Magnetic Suspensions with Rheological, Magnetic, Electrical, and Thermal Reinforcement, *ACS Appl. Mater. Interfaces*, 2021, **13**, 5256–5265.

41 B. Priyanuj, Y. W. Wei, D. H. Sin, J. S. Yu, C. W. Nah, K. U. Jeong, D. D. Michael and S. J. Park, Soft and Stretchable Liquid Metal Composites with Shape Memory and Healable Conductivity, *ACS Appl. Mater. Interfaces*, 2021, **13**, 28916–28924.

42 W. Wang, Z. M. Fan, J. F. Wang, C. Wu, J. X. Tang, L. Tang, D. J. Zhang, Z. M. Xie, Z. J. Cheng and Y. Y. Liu, Highly Conductive Liquid Metal-Based Shape Memory Material with an Ultrasensitive Fire Warning Response, *ACS Appl. Polym. Mater.*, 2021, **3**, 6027–6033.

43 S. Chen, R. Q. Zhao, X. Y. Sun, H. Z. Wang, L. Li and J. Liu, Toxicity and Biocompatibility of Liquid Metals, *Adv. Healthcare Mater.*, 2023, **12**, 2201924.

44 Q. Liu, S. S. Meng, T. T. Zheng, Y. M. Liu, X. Ma and H. H. Feng, Alkaline-Driven Liquid Metal Janus Micromotor with a Coating Material-Dependent Propulsion Mechanism, *ACS Appl. Mater. Interfaces*, 2021, **13**, 35897–35904.

45 H. D. Lu, G. L. Yun, C. Tim, Y. M. Ouyang, H. T. Ren, J. Shu, Y. X. Zhang, S. W. Zhang, D. D. Michael, W. H. Li and S. Y. Tang, Reversible Under-water Adhesion for Soft Robotic Feet by Leveraging Electrochemically Tunable Liquid Metal Interfaces, *ACS Appl. Mater. Interfaces*, 2021, **13**, 37904–37914.

46 D. D. Xu, J. Hu, X. Pan, S. Sánchez, X. H. Yan and X. Ma, Enzyme-Powered Liquid Metal Nanobots Endowed with Multiple Bio-medical Functions, *ACS Nano*, 2021, **15**, 11543–11554.

47 Z. L. Wang, X. H. Wang, Q. Miao, F. F. Gao and Y. P. Zhao, Spontaneous Motion and Rotation of Acid Droplets on the Surface of a Liquid Metal, *Langmuir*, 2021, **37**, 4370–4379.

48 S. Y. Wang, Z. Q. Zhu, C. Z. Ma, R. Qiao, C. Y. Yang, X. X. Ronald and S. Ting, Generation of Nonspherical Liquid Metal Microparticles with Tunable Shapes Exhibiting an Electrostatic-Responsive Performance, *ACS Appl. Mater. Interfaces*, 2021, **13**, 16677–16687.

49 F. R. Meng, F. Q. Wang, H. H. Yu, Z. J. Zhao, L. Yang, M. Chao, D. Zhang and X. Z. Liu, Liquid Metal-Modified Nanoporous SiGe Alloy as an Anode for Li-Ion Batteries and Its Self-Healing Performance, *ACS Appl. Energy Mater.*, 2021, **4**, 14575–14581.

50 J. X. Zhang, Q. Y. Lu, Y. Y. Li, T. Y. Li, M. H. Lu, Y. F. Chen and D. S. Kong, An Ultrastretchable Reflective Electrode Based on a Liquid Metal Film for Deformable Optoelectronics, *ACS Mater. Lett.*, 2021, **3**, 1104–1111.

51 Z. Ma, Q. Huang, Q. Xu, *et al.*, Permeable superelastic liquid-metal fibre mat enables biocompatible and monolithic stretchable electronics, *Nat. Mater.*, 2021, **20**, 859–868.
52 J. Tang, S. Lambie, N. Meftahi, *et al.*, Unique surface patterns emerging during solidification of liquid metal alloys, *Nat. Nanotechnol.*, 2021, **16**, 431–439.
53 S. F. Aleksandra, K. K. Nikita, V. B. Semyon, A. M. Valentin and V. V. Vladimir, Single Particle Color Switching by Laser-Induced Deformation of Liquid Metal-derived Microcapsules, *J. Phys. Chem. Lett.*, 2021, **12**, 7738–7744.